

# Tomography

*Prabhat Munshi*



Prabhat Munshi is a Professor of Mechanical Engineering at IIT Kanpur. His major areas of his interest are computerized tomography and nuclear reactor safety analysis.  
<http://home.iitk.ac.in/~pmunshi/>

**Tomography is traditionally associated with medical ‘CT’ scanners that have been in use for over 30 years now. This mathematical concept is now applied widely by scientists and engineers in a variety of measurements involving solids, fluid, gases and plasmas. Instrumentation based on X-rays, gamma-rays, lasers and acoustics have been used successfully in these applications. Inherent error in such measurements can be also be estimated thus making tomographic imaging a very powerful non-invasive technique for field measurements.**

The concept of tomography involves (a) ‘seeing’ inside optically opaque solid objects without cutting them, and (b) making measurements inside a non-solid system in a non-invasive manner. The advent of computers resulted in renaming of this concept as ‘computerized tomography’ and is abbreviated as CT. The most popular application of CT has been in the field of medical diagnostics where it was known as X-ray ‘CAT Scan’ during 1970s. The inventor of this imaging machine, G.N. Hounsfield, was awarded the Nobel Prize in 1979 along with A. Cormack who demonstrated that the mathematics behind tomography is indeed applicable for real objects. The social contribution to X-ray CT scanners is immense as medical experts can image organs at a much higher spatial resolution compared to conventional X-ray scanners and to even diagnose cancer at an early stage.

Hounsfield [1] used the techniques of linear algebra to obtain CT images from tomographic measurements, known as ‘projections’. Fourier based methods of image reconstruction were not used due to difficulties in the numerical implementation of the algorithm. Around the same time, Ramachandran and Lakshminarayanan [2] published an alternative method for producing CT images from projection data (*Figures 1 and 2*). This landmark paper revolutionized the medical imaging field and all major manufacturers

## Keywords

Tomography, projection.



## Convolution Back Projection

(G. N. Ramachandran and A. V. Laxminarayanan, 1970)

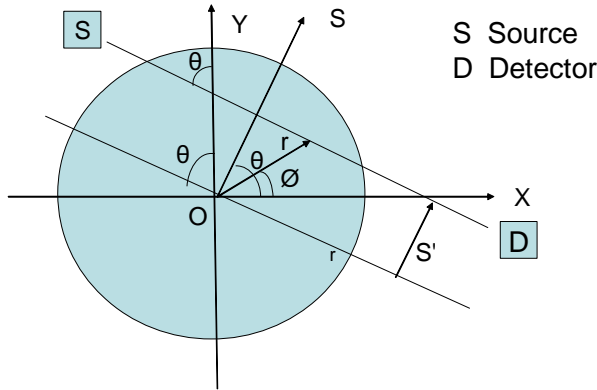


Figure 1 (top). Data collection geometry for a parallel beam CT scanner. The chord SD represents one data-ray. There will be several such rays for different values of  $s$ , the perpendicular distance of the data-ray from the origin. The source-detector system rotates and  $\theta$  is the angle of rotation. For every  $\theta$ , we have rays corresponding to various values of  $s$ .

## Convolution back projection

- The **Radon transform** representing the projection data is

$$p(s, \theta) = \int_{SD} f(r, \phi) dz$$

- Implementing the **projection slice theorem**, which represents the equivalence of 2D Fourier transform of object function  $f(r, \phi)$  and 1D Fourier transform of projection data  $p(s; \theta)$ , we get

$$\hat{p}(R, \theta) = \hat{f}(R \cos \theta, R \sin \theta)$$

Figure 2 (bottom). This is the Central Slice Theorem that relates the data collected in Figure 1 to the cross section  $f(x, y)$  that generates the data.  $R$  is the Fourier frequency.

of medical CT scanners switched to this new algorithm that is now known as the convolution backprojection technique (CBP) (Box 1, Figures 3-5). It is very fast, easy to implement and very simple to understand.

This powerful, nondestructive imaging technique captured the imagination of materials science and engineering groups during the 1980s. These groups developed specialized CT using machines to image objects in micrometer scales ( $\sim 20 \mu\text{m}$ ) and were known as micro-CT scanners. Within a decade, micro-CT scanners became an integral part of the leading nondestructive testing



**Box 1. CBP Algorithm.**

Here we review CBP briefly.

The CT projection data denoted by  $p(s, \theta)$  given by

$$p(s, \theta) = \int_{SD} f(r, \phi) dz \quad (A1)$$

where  $s$  is the perpendicular distance of the ray from the object centre and  $\theta$  is the angle of the source position.

Using this data, the reconstructed function  $\tilde{f}(r, \phi)$  is evaluated by the equation

$$\tilde{f}(r, \phi) = \int_{0-\infty}^{\pi \infty} p(s, \theta) q(s' - s) ds d\theta \quad (A2)$$

where

$$q(s) = \int_{-A}^A |R| W(R) e^{i2\pi RS} dR \quad (A3)$$

is known as the convolving function and  $s'$  is the data ray passing through  $f(r, \phi)$ , the point being reconstructed,  $R$  is the Fourier frequency,  $A$  is the Fourier cutoff frequency and  $W$  is the filter function which is user dependent (see *Figure 5*). Different filter functions give different reconstructions for the same data set. For medical imaging, Hamming filters are popular.

In the present work, medical images are given as input for the reconstruction. The algorithm first extracts the projection data through inbuilt radon function from the medical images. This projection data is then used to reconstruct the images using convolution back projection (CBP) method. Once the reconstruction is done, the error incurred in reconstruction is estimated.

Figure A shows the effect of filters in CBP algorithm. The CT images included here are from a gamma-ray tomography experiment (carried out at Bhabha Atomic Research Centre, Mumbai) for a steady state two-phase mercury-nitrogen flow.

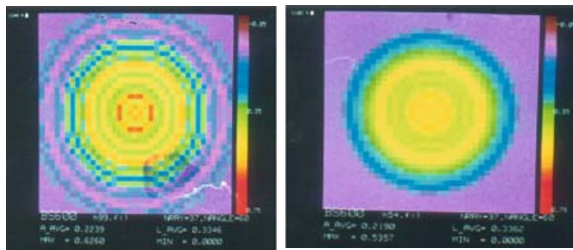


**Figure A. Different windows (filters),  $W(R)$ , result in different CT images as per Figure 4. Both are correct (mathematically) solutions. The user has to pick the right solution based on additional information. In case the conditions of the error formula (Eq. B1 in Box 3) are satisfied, it can be used to pick the 'right' solution from a set of 'correct' solutions.**

(NDT) groups all over the world. Tomography has also been used to study plasma properties and measurement of temperature profiles in gaseous medium. The first attempt to use this concept



## Convolution Back Projection

- 2D inverse Fourier transform of projection data gives tomographic inversion formula

$$f(r, \phi) = \int_0^{\infty} \int_{-\infty}^{\infty} p(R, \theta) e^{i2\pi Rr \cos(\theta - \phi)} |R| dR d\theta$$

where, 
$$\hat{p}(R, \theta) = \int_{-\infty}^{\infty} p(s, \theta) e^{-i2\pi R s} ds$$

- $f(r, \phi)$  in the inner integral is divergent, and thus requires a smarter solution for practical implementation
- It is achieved through the use of filter functions which introduce frequency band-limitation.

## Convolution back projection

- The approximate form of  $f(r, \phi)$ , after introduction of the filter function, becomes

$$\tilde{f}(r, \phi) \approx \int_0^{\infty} \int_{-\infty}^{\infty} \hat{p}(R, \theta) e^{i2\pi Rr \cos(\theta - \phi)} |R| W(r) dR d\theta$$

where, 
$$W(R) = 1, |R| \leq R_c$$
  

$$= 0, |R| > R_c$$

(Ram-Lak filter)

*Figure 3 (top). The CBP algorithm as implemented in IISc by (late) Prof G N Ramachandran in 1969.*

*Figure 4 (bottom). The variation in CBP introduced later enhancing the range of application of CBP algorithm. The window function  $W(R)$  is also known as filter function. The special case of this filter is the Ramachandran–Lakshminarayanan filter abbreviated as Ram–Lak filter in CT literature.*

in two-phase air-water flows was demonstrated in 1979-80. All these groups were working with the same mathematical concepts without knowing about the existence of each other. This awareness spread only during the 1990s, but tomography started becoming popular in India only after about 20 years after the publication of the landmark paper from Indian Institute of Science [2].

Different types of instruments are being used in tomographic measurement and imaging exercises. The ‘big four’ players are instruments involving X-rays, gamma-rays, acoustics and lasers. The medical CT scanners use X-rays, the industrial NDT tomo-

Different types of instruments are being used in tomographic measurement and imaging exercises. The ‘big four’ players are instruments involving X-rays, gamma-rays, acoustics and lasers.



Figure 5. The two mathematical steps of CBP.

## Convolution back projection

- Using the convolution theorem of the Fourier transforms, we get

$$\tilde{f}(r, \phi) \approx \int_0^{\pi} \int_{-\infty}^{\infty} p(s, \theta) q(s' - s) ds d\theta$$

One dimensional **convolution**

$$q(s) = \int_{-\infty}^{\infty} |R| W(R) e^{i2\pi Rs} dR$$

Averaging over  $\theta$ ,  
termed as **back projection**

graphic set-ups primarily employ X-ray and gamma-rays. Acoustic CT machines are still being developed for several applications for material testing (in the frequency range of 1-10 MHz, hence called ultrasonic CT) and ocean diagnostics (range, kHz). Thermal imaging and microwave imaging have also been explored and is slowly catching up with the ‘big four’.

The key feature of all CT instruments is the underlying mathematics that is independent of the physics involved. Measurements are made, in general, on a 2-D plane and the data collected is a set of line-integrals of a particular ‘physical’ property, say,  $f(x, y)$ , of a cross-section of the object being investigated. The tomographic algorithms accept these line-integrals (known as ‘projection data’) as input and estimate the unknown function  $f(x, y)$  (Figure 5). In NDT and medical applications with X-rays,  $f(x, y)$  is the absorption co-efficient of the X-rays (photons) and can be related to the density of the object. When we use lasers to measure the temperature fields of gaseous objects,  $f(x, y)$  is the refractive index of the medium (gas) and is related to the temperature. Similarly for acoustic applications,  $f(x, y)$  plays the role of  $1/v$ , known as ‘slowness’, where  $v$  is the speed of sound in the medium.



We also mention here that lasers are being used in three different modes: interferometry<sup>1</sup>, Schlieren<sup>2</sup> and shadowgraph<sup>3</sup>. The difference in the physics of these techniques does not change the mathematical algorithms. It only affects  $f(x, y)$ . For interferometry,  $f(x, y)$  is refractive index,  $n(x, y)$ , as mentioned above. For Schlieren and shadowgraph, it is the first and second derivative, respectively, of the refractive index with respect to the direction perpendicular to that of the laser beam. In acoustics, time-of-flight tomography has already been mentioned above. The other popular option is the ‘amplitude’ and ‘phase’ tomography<sup>4</sup> and the attenuation properties of the energy of the acoustic/optical wave.

We can also classify CT techniques based on the inherent nature and physics of the signal used e.g. transmission, emission, reflection and diffraction. In medical imaging, the popular X-ray CT machine is in the transmission mode. On the other hand, the medical PET<sup>5</sup>/SPECT<sup>6</sup> machines belong to the emission category, where the aim is to reconstruct the photon/positron emission sources using estimates made externally (see *Box 2*.) The other popular application of emission tomography is in the area of plasma diagnostics where soft X-ray emissions from the plasma field are measured by detectors located outside the fusion reactor.

Applications of CT are widespread in many other areas such as, astrophysics (study of the corona of the sun), ocean science (salt content), atmospheric science (water-vapour distribution), archeology (identification of elements from the metallurgical point-of-view), geophysics (identification of oil/rocks), molecular biology (structural details) and most recently nanotechnology. The challenge, however, is that only one CT machine (based on ion-beam technology) is operational in the world (at Los Alamos) and the resolution reported is around 50 nm. It may be mentioned here that the highest resolution an X-ray CT scanner can image is 10  $\mu\text{m}$  and the state-of-the-art medical CT scanners provide 500  $\mu\text{m}$  in-plane spatial resolution.

In India, we have about 10 experimental groups that work on

<sup>1</sup> **Interferometry:** A laser based technique that involves interference of two coherent light waves (<http://en.wikipedia.org/wiki/Interferometry>).

<sup>2</sup> **Schlieren:** It is a distortion based phenomenon involving the first derivative of refractive index ([http://en.wikipedia.org/wiki/Schlieren\\_photography](http://en.wikipedia.org/wiki/Schlieren_photography)).

<sup>3</sup> **Shadowgraph:** It involves the second derivative of refractive index (<http://en.wikipedia.org/wiki/Shadowgraph>).

<sup>4</sup> **Amplitude and Phase Tomography:** Signals have a phase and amplitude and this information can be used separately to measure physical properties. Optical coherence tomography is one such example.

([http://en.wikipedia.org/wiki/Optical\\_coherence\\_tomography](http://en.wikipedia.org/wiki/Optical_coherence_tomography)).

<sup>5</sup> **PET:** Positron Emission Tomography.

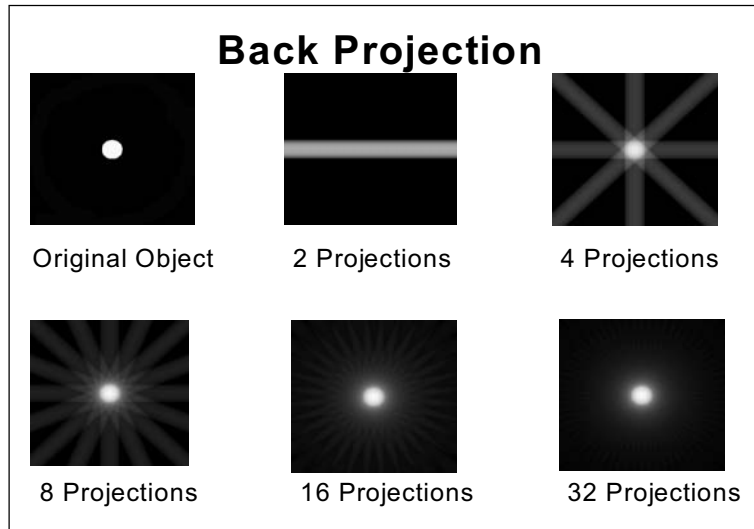
<sup>6</sup> **SPECT:** Single Photon Emission Computed Tomography.

#### Box 2.

Positron Emission Tomography: Patients are given a dose of radioactive liquid that emits positrons. They escape the human body and get captured by suitable detectors placed outside the patient. It results in a tomographic image that gives the distribution of the blood flow in the organ being investigated.



**Figure 6.** The image,  $f(x,y)$ , improves when the numbers of projections are increased. The star like artifacts disappear as the discrete form of the double integral (of Figure 4) approaches the exact value.



X-rays, gamma rays, lasers and ultrasound tomography [3]. The most accurate one is the X-ray/gamma-ray but it is very expensive and not very attractive from the social acceptance point-of-view. Laser techniques have limited applications and require sensitive working environments. Acoustic equipment is not expensive and socially acceptable but the underlying mathematics is non-linear, implying the need for a highly trained user to get any meaningful results.

Finally, we talk about the accuracy of the CT images. Ramachandran and Lakshminarayanan method (CBP algorithm) is the one algorithm that is used widely all over the world in medical and industrial CT scanners (*Figures 1–6*). Natterer [4] introduced Sobolev space theory in developing error analysis theorems for CT images. Munshi *et al* [5] followed this work and carried out a precise quantification of these errors resulting in an approximate error formula for the CBP algorithm [6]. This formula was verified numerically [7] as well as experimentally on three different CT scanners located in Germany, Australia and England [8–10]. We thus now have precise prediction of error for the CBP algorithm. This gives additional information to the users [11] about the accuracy of the CT images produced by CT machines available commercially. *It also provides a very interesting*



**Box 3. Approximate Error Formula**

The inherent error incurred is strictly due to finite cut-off,  $A$ , of the Fourier frequency and is precisely zero if the projection data happens to be band-limited and the cut-off frequency is chosen to be the highest frequency contained in  $p$ . In general, to avoid aliasing artifacts the choice,  $A=1/(2\Delta s)$ , is recommended. Here  $\Delta s$  is the spacing of the data rays.

It has been shown that simplified form of  $E$  at a given point  $f(r, \phi)$  in the object cross-section, is given by,

$$f(r, \phi) - \tilde{f}(r, \phi) \equiv E(r, \phi) = k(W''(0))(\nabla^2 f(r, \phi)) \quad (B1)$$

$$\text{where } W''(0) = \left. \frac{\partial^2 W(R)}{\partial R^2} \right|_{R=0} \quad (B2)$$

$\nabla^2 f$  is the Laplacian of  $f$  and  $k$  is a constant depending on the data ray spacing. The above error formula is local by nature and predicts error on a pixel-by-pixel basis. It is more useful to have an 'error' estimate associated with the whole image rather than on a pixel-by-pixel basis. It has been shown that if  $NMAX$  represents the maximum value of gray-level in reconstructed image then  $1/NMAX$  is an indicator of overall error incurred in reconstruction. This method is useful for error estimation even if the original object is unknown. *Figure 1* gives the parallel-beam data collection geometry.

*estimate of errors in CT measurements even when the original cross section is not available.* This quantification of error can be used to monitor the progress of cancer patients undergoing treatment and some initial results are also available [12]. A brief summary of the error formula is given in *Box 3*.

We see that tomography has captured the imagination of researchers cutting across various disciplines and has proven to be the only option in many cases as far as non-invasive measurements are concerned. The combination of CT scanners and error estimates will provide very interesting quantitative information to various experts who are using, or intend to use tomography in a very meaningful manner.

**Suggested Reading**

- [1] G N Hounsfield, **Computerized transverse axial scanning (tomography). 1. Description of system**, *Br. J. Radiol.*, Vol.46, pp.1016–1022, 1973.



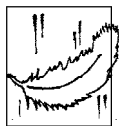


**Acknowledgement**

Mr Sunil Verma, RRCAT, Indore  
for Figures 1–6.

- [2] G N Ramachandran and A V Lakhshminarayanan, Three-dimensional reconstruction from radiographs and electron micrographs: Application of convolution instead of Fourier transforms, *Proc. Natl. Sci. Acad. USA*, Vol.68, pp.2236–2240, 1971.
- [3] P Munshi (ed.), *Computerized Tomography for Scientists and Engineers*, CRC Press, New York 2007.
- [4] F Natterer, *The Mathematics of Computerized Tomography*, John Wiley & Sons, New York, Equation 4.6, p.139, 1986.
- [5] P Munshi, R K S Rathore, K S Ram and M S Kalra, Error Estimates for Tomographic Inversion, *Inverse Problems*, Vol.7, pp.399–408, 1991.
- [6] P Munshi, Error analysis of tomographic filters I: Theory, *NDT & E International*, Vol.25, pp.191–194, 1992.
- [7] P Munshi, R K S Rathore, K S Ram and M S Kalra, Error analysis of Tomographic filters II: Results, *NDT & E International*, Vol.26, pp.235–240, 1993.
- [8] P Wells and P Munshi, An analysis of theoretical error in tomographic images, *Nuclear Instruments and Methods in Physics Research*, Vol.B93, pp.87–92, 1994.
- [9] P Munshi, M Maisl, H Reiter, Experimental aspects of the approximate error formula for computerized tomography, *Materials Evaluation*, Vol.55, pp.188–191, 1997.
- [10] G Davis, P Munshi, J C Elliott, Analysis of hard biological tissues using the tomographic error formula, *Journal of X-ray Science and Technology*, Vol.6, pp.63–76, 1996.
- [11] P Munshi, Picking the right solution from a set of correct solutions, *Measurement Science and Technology*, Vol.13, pp.647–653, 2002.
- [12] Mayuri Razdan, Amit Kumar and P Munshi, Second Level KT-1 Signature of CT Scanned Medical Images, *Int. J. Tomography and Statistics*, Vol.4, pp.20–32, 2006.
- [13] G T Herman, Image reconstruction from projections: *The Fundamentals of Computerized Tomography*, Academic Press, New York, 1980.
- [14] A C Kak and Malcolm Slaney, *Principles of Computerized Tomographic Imaging*, IEEE Press, 1988. Free electronic copy available for download at <http://www.slaney.org/pct/pct-toc.html>,

Address for Correspondence  
Prabhat Munshi  
Department of Mechanical  
Engineering  
Indian Institute of Technology  
Kanpur 208 016, India.  
Email: pmunshi@iitk.ac.in



### Prof G N Ramachandran and Tomography

Some of the early work on the mathematical methods of tomography was carried out by Professor G N Ramachandran during the early seventies. “Literature on that subject acknowledges GNR’s contributions both directly and intentionally by citing his pioneering articles and as well as indirectly and unintentionally by using the notation  $G_n(R)$  for the density function that describes the object”. (N V Joshi, *Resonance*, Vol.6, No.10, pp.92–96, 2001.)

